Recent trends and emerging challenges in two-dimensional materials for energy harvesting and storage applications

Introduction

1/3 dimensions may be nanoscale, 4 types of nanomaterials:
- 3D: 3 dimensions > nanosize, can be seen by naked eye
- 2D: 1 dimension nanosized, for eg nanosheets
- 1D: 2 dimension nanosized, 1D in cm/mm, for eg nanotube
- 0D: All 3 dimensions nanosized, for eg quantum dot

Some 2D materials: graphene, Xenes, phosphorene, tinene germanene, antimonene, borophene, stanene, silicene

Some types of 2D materials

Graphene
- 1st modern 2D element
- 1-atom thick covalently bonded hexagonal lattice of C atoms
- Highest tensile strength
- Unique band structure thus, thermal conductivity

2D TMDCs
- Chemical formula MX_2 X=chalcogen (S/Te/Se) M=transition metal (Mo)
- Indirect bandgap in bulk
- Optoelectronics - direct BG in visible spectrum
- Charge transistor - charge mobilities

Hexagonal boron nitride
- Graphene isomorph: B & N atoms replacing C
- Wide-bandgap insulator

Xenes
- Group of Si/Ge/Sn MLs
- Graphene isomorph but buckled to certain degree
- Epitaxially grown on substrate, not exfoliated

Phosphorene
- Stable layered elemental P allotrope direct bandgap
- Ideal for optoelectronic devices-high charge mobility

Synthesis of 2D

If material with 3D oriented molecular bonds slimmed to 2D, high density of chemically unstable hanging bonds created, rearrangement of shape req to lower surface energy.
Top down synthesis: Mechanical/Liq exfoliation; Bottom down synthesis: CVD, chem. synthesis
- Mechanical exfoliation: Sticky tape used to peel layers; low ML yield, low shape/size control
- Liq exfoliation: In irganic solvent medium, sonication makes layers separate via tensile stress
- Chemical synthesis: interface-mediated growth, nanoparticle fusion into bigger nanosheets, etc. most scalable, low-cost, and flexible approach for large-scale
- CVD: heated furnace to pass precursor gases through, where they combine or with a substrate to form thin layer of material; more complex and expensive, but scaleable

Energy applications of 2D materials

Used where bulk materials unsuitable due to change in properties due to reduction in dimensionality

Sensors and transistors
- 2D FETs - high charge mobility + low BG
- H-BN – gate dielectric; Graphene - active channel in transistors by opening bandgap
- FET-based sensors from 2D TMDCs can detect range of chemicals in ppm range

Battery electrodes
- Electrodes for ion batteries require electrical conductivity with large surface area to store high densities of ions
- Graphene: higher surface-mass ratio, high conductivity, greater mech strength, flexibility
- 2D MoS_2: potential electrode as it adopts metallic 1T phase by chemical exfoliation

Photodetectors
- TMDCs: Optical or near-infrared bandgap and good charge transport properties
- 1 ML of TMDC absorbs ~10% of incident visible light, sufficient for photo detectors

Nanogenerators
- Odd layer TMDCs have piezoelectric properties (absence of inversion symmetry)
- If substrate bent at ends, MoS_2 flake expands, causing piezoelectric charges at edges, driving e^- flow in an external circuit
- Some 2D materials have piezoelectricity + mechanical flexibility; can be used for wearable power generating nanodevices

Observation of single-defect memristor in an MoS2 atomic sheet

Introduction

- Non-volatile resistive switching: electric field switches resistance states of two-terminal device
- High-density information storage computing & reconfigurable systems could use memristor effect but it was believed leakage currents would prevent this for 1nm-thin insulating layers until its discovery in 2D monolayers of transition metal dichalcogenide & hexagonal boron nitride
- Metal substitution into S vacancy results in non-volatile change in resistance, supported by computational studies of defect structures
- New direction in precision defect engineering, down to a single defect, towards achieving the smallest memristor for applications in ultra-dense memory & neuromorphic computing

Preparation

- MoS_2 monolayers prepared by exfoliation onto Au surfaces & annealed@250^{o}C for hours in ultrahigh vacuum conditions
- Gold STM tip used as top electrode for transport, fixed on surface and moved towards MoS_2 for 2-4 Å for stable contact

Why MoS_2

- Formation energies of defect critical to stability & transitions & MoS2 V_S & V_{S2} have low EOF of 1.3-2.9eV & 2.9-5.9eV
- Density of V_s globally altered by annealing in a vacuum or S-rich atmospheres
- Enhanced fields allow migration of Au to or from defect, hence stable reversible reaction
- Due to layered structure, MoS_2 provides sharp, clean interface to prevent excessive tunnelling current but allows adatoms from electrodes to be absorbed in vacancy sites

Observations

- From STS-STM & local transport studies, S vacancy (V_s) shows no low-resistance path in its native form until substituted by M^+ ions (gold) resulting in conducting LDOS, creating low resistance state. After removal of M^+, defect recovers & restores high resistance
- STS shows bandgap less than optical bandgap due to charge transfer from Au substrate & reveal V_s don't enhance tunneling current
- Transport meas. reveal tunneling-like I-V phenomena on defect-free zone & repeating transport measurements around defect sites reveal unipolar diode-like behaviour with suppressed charge transport for positive tip biases possibly due to charge accumulation
- I–V curves (110M-2.5GΩ) similar to resistive switching observed at V_s; Switching can induce new defects & change gold terrace structure
- STM shows V_{S2} defect with triangular symmetry, darker contrast & bandgap similar to defect free. V_S:V_{S2}=10:1. Repeated measurements trigger switching events and then STM images are taken which show that dark spot is replaced by bright protrusion of ~0.5 Å height
- Stability & height of bright spot indicate substituent in vacancy and STS shows non-zero DOS at Fermi level, revealing metallic behavior
- DFT-based 1st principle calculations for Au-MoS_2-Au models & Green's function reveal that gold-ion adsorption into divacancy causes change in I
- Subsequent transport measurements with an opposite tip bias trigger a second resistive switching event from low to high resistance

A sub-500 mV monolayer hexagonal boron nitride based memory device

Abstract

- Ultrathin 2D nanomaterials, such as graphene and transition metal dichalcogenide (MoS_2, WS_2, TiS_2, TaS_2) have raised increasing attention for RRAM
- Ultrathin layer offer low working voltage, ultra-dense integration, high-speed switching
- Transfer and lithography-free resistive switching device based on CVD grown h-BN vertically sandwiched by different metallic electrodes reported in this paper
- Low operating voltage (<.5V), large on/off ratio, long retention time, excellent flexibility
- Tunneling conduction shown in off & on-state current conducts via metallic conducting filaments formed by the substitute of metal ions for lattice vacancies in h-BN
- Polymer layer inserted to constrain conducting filament size and block the formation of unwanted filament from Cu bottom, to obtain monolayer h-BN resistive memory device

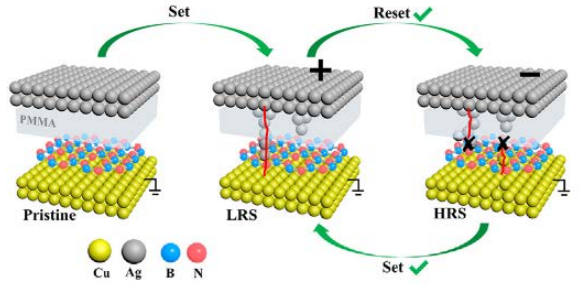

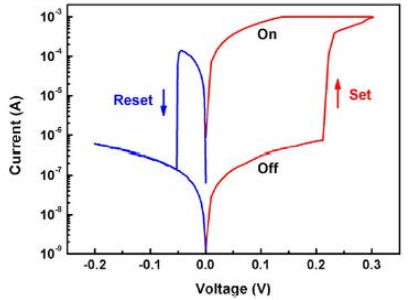

Experimental

- CVD-grown monolayer h-BN bought from 6Carbon Technology
- VASP for DFT based on pseudopotential plane-wave method

Observations

- Initial high resistance state (HRS) switches to low resistance (LRS) at ~1 V during the 1st sweep, but doesn't switch back as only partially reset by 3rd sweep
- Thin PMMA inactive layer (~ 10 nm) with low processing temp, low cost, high resistivity inserted between top electrode (TE) and h-BN to reduce reset current
- Au TE device has higher working current, small on/off ratio (<10). Ag/Cu TE preferable for memory device in light of energy efficiency and data robustness
- On measuring Ag/PMMA/Cu structure, +ve sweep shows increase in current at .4V, but negative sweep can't reset it, thus CuO and PMMA layer affect switching
- Fitting of +ve sweeping region shows linear charge transport at LRS & HRS but only LRS is temperature dependent, indicating metallic conducting filament (CF)
- RS supported by ABS: B vacancies found mainly at grain boundaries. In simulation, Ag/Cu ions placed near h-BN nanosheet with B vacancy, and after structure optimization calculation, Ag/Cu ion fills boron vacancy on the h-BN layer. Ag dopants cause local deformation of lattice but maintained main morphology of lattice
- Ag atoms are isolated and introduce flat bands (localized states) in band gap, leading to a DOS peak at Fermi energy level. By increasing replacement to 6.25%, adjacent Ag begin to interact, bending flat bands in band gap, & at 11.1%, cross the Fermi level, leading to partially-filled band (e^- contribute to conductivity)
- In devices without PMMA, Ag and Cu ions, from TE and BE respectively, are chemically active to fill B vacancies, thus reset tough for Ag/h-BN/Cu structure
- PMMA prevents overgrowth of CF & helps block formation of Cu filaments during reset process, which improves the device yield and switching reliability
- Sub-nm thinness & high breaking strain of monolayer h-BN make device highly desirable for flexible nonvolatile memory, functioning perfectly upto 2% strain
- Ultra-low working voltage may be useful for unconventional applications like mobile computing or medical devices, using person's body temperature or exercise to meet power needs due to low power consumption, although endurance & switching uniformity not yet sufficient to meet critical requirements for digital memory

Imaging and identification of point defects in $PtTe_2$

1. PtTe2 film synthesis and characterization

- Deposition of Pt & Te layers by sputtering and electroplating, annealing of sample at 450 °C for 1.5hr to synthesize PtTe2 film
- XPS to confirm successful synthesis of film and assess quality
- Raman spectroscopy to study quality of the material synthesized
- XRD to examine film crystallinity, indicated by sharp peaks in
- SEM images show polycrystalline nature with 200-400nm grains

2. STM characterization of point defects

- Average lattice constant and layer step height of 4.0 and 5.1 Å
- According to STM, thickness of flakes ranged 30 - 50 layers
- Bigger defects appear less bright, correlated with defect depth
- 5 types of defects: A,B,C,D,E. A show depressions at both bias voltages, rest display protrusions (depressions) at –ve (+ve) bias
- A, C most common, supported by calc. defect formation energy
- B are 6 × 6 triangular depression at +ve bias. At -ve bias, defect is characterized by small protrusion of the same triangular area
- C are 3 × 3 triangular depression at +ve bias voltage and a small depressed triangle flanked by 3 protruding spots at negative bias
- D has hexagonal depressions at +ve bias & completely changes in shape to 3 triangular small inward-pointing depressed triangles
- E is 3×3 triangular depression (protrusion) at +ve (-ve) bias voltage and is an antisite defect with Te replacing Pt

3. STS characterization of defect-free area & defects

- Defect edge shows higher LDoS than flat defect-free area as Te vacancy creates high acceptor density resulting in triangular shape

Abstract

- Type-II Dirac high conductivity semimetal, maybe for spintronics, quantum computing
- Point defects can be interstitial, vacancies, self-interstitial, substitutional or a mix
- STM to resolve atomic structure/point defects non-destructively & STS to study LDOS
- Tip modeled as locally spherical potential well and tunneling current ∝ LDoS, at the position of the tip where it approaches nearest to the surface, assuming that tip wave function has s-orbital character, at distances away from surface, partial density will be zero for localized basis set calculations since the basis orbitals have a finite range
- Following Raman spectroscopy, XPS, XRD & SEM, STM and STS done with DFT

4. Electronic structure of PtTe2

- Band structures of monolayer (ML), bilayer (BL), and bulk PtTe2 via generalized gradient approximation (GGA) and GGA-1/2, considering spin–orbit coupling (SOC)
- Indirect bandgap increases for GGA-1/2, comparable to bandgap of semiconductors, thus ML PtTe2 of interest for electronics like FETs, where effect of dopants is critical
- GGA-1/2 “flattens” curvature of VB, pushing CB up in energy; increasing bandgap
- Energy level of VBM exceeds CBM, hence overlap of bands, hence semimetal-semiconductor transition occurs due to quantum confinement, showing BL PtTe2 metallic
- In ML, BL, bulk PtTe2, p and d orbitals contribute equally to CB, VB originate from p-orbitals compared to d-orbitals, with 10x less contribution from s-orbitals
- For Te vacancy, Fermi level is at mid-bandgap; for Pt, in the lower half of the bandgap
- Large spin-orbit splitting in defect states, making PtTe2 good for spintronic applications

5. Defect formation energy

- Formation energies of Te, Pt vacancy calculated by: $E_f=E_{tot}(defect)-E_{tot}(pristine)+\Sigma N\mu_i$
- When Te-rich, μ_{Te} calculated from Te energy in bulk; when Pt-rich, $\mu_{Te}=0.5\times(\mu_{PtTe2}-\mu_{Pt})$
- When Pt-rich, μ_{Pt} calculated from Pt energy in bulk; when Te-rich, $\mu_{Pt}=\mu_{PtTe2}-2\times\mu_{Pt}$

Rise of the Xenes: From the Synthesis to the Integration Processes for Electronics and Photonics

1. Xenes Background and State-of-the-Art

- Possible to arrange Si and Ge a honeycomb lattice inspite of increased atomic mass wrt C as lattice undergoes buckling. Degree of buckling can be tuned, with low-buckled being stable than high-buckled configurations
- Even if freestanding silicene and germanene can exist, no bulk Si, Ge crystals made of silicene and germanene slices to be peeled off
- Noble metals like Ag (111) surface substrate to host large no of Xenes: Using molecular beam epitaxy (MBE), silicene, germanene, stanene, borophene, antimonene were successfully realized
- Choice of substrate important as it determines properties of deposited Xene, via chemical interaction between X atoms and substrate
- Various electronic states makes Xenes appealing for device applications
- Advantage of monoelemental crystals: easier characterization independent of environment + provides opportunity of assembling new materials
- Challenges of Xenes: large scale deposition with easier, cheaper tools; instability of many Xenes, technology readiness level needs to be raised

2. Electronic properties

- Thickness/roughness of 2D materials controlled accurately, thus reliability and uniformity of electronic devices optimizable. Since graphene, 2D material FETs report ON/OFF current ratios >107, subthreshold swing ~62mV/decade
- Silicene FETs suffer from limited lifetime (~2 days) at ambient conditions
- Study req on transfer process or lithographic step to provide nm resolution
- Surface termination can tune optical and electronic properties, improving stability
- Group 16 FETs exhibit p-type transport due to presence of H & OH terminations on the nanosheets surface, with high ON/OFF current ratio and hole mobility; act like semi-conductors, making it appealing for electronic applications

4 conditions to provide useful technological knowledge on the Xenes-based FETs

- Methods of Xenes synthesis & device fabrication must be scalable to wafer level
- Morphology and density of non-idealities in Xenes specified (lattice distortions)
- FET size small enough to be compatible with integration density requirements
- Information about yield, device-to-device variability, reliability & stability provided

Future challenge: Improving performance; extend fabrication methods to all Xenes

3. Photonics Applications

- Novel optical responses from material engineering, controlling thickness or morphology manipulation and realization of 2D heterostructures
- Calculated optical properties of 2D silicene revealed spectral features absorbance like graphene due to linear bands & Dirac cones at low optical frequencies, interband transitions near critical points higher photon energies
- In IR range of 2D silicon, Dirac-like absorption resembling silicene (theoretical)
- Can exploit non-trivial topological state in plasmonic optical response in ultrathin tin nanosheets. QSH insulator state expected in stanene/silicone
- Combining optical + electronic properties key for photonic devices
- Non-linear optical properties: nonlinear photodiode, Q-switching, modulators
- Xenes intergration adds complexity in design due limitations in synthesis

4. Challenges and Advances in Xene Processing

- For complex device architectures, control of Xene quality must be improved

Further investigations req. in compatibility with standard nanofabrication tools

- Establish patterning/etching protocols assessing stability & response of various Xenes to chemicals and physical agents, like annealing, etching, deposition
- In-situ encapsulation of silicene via Al_2O_3 capping layer protects silicene in ambient condition & enables electrostatic gating of Xene-based FET channels
- Capping layer engineering needs to be proposed, exploiting novel materials

Transfer of Xene (native->arbitrary substrates) needed; depends on crystal orientation

- Novel methods needed where a Xene layer forming heterostructure is considered as sacrificial aiming at improving the reliability of the transfer process

Progress on learning modelling softwares

1. Quantum Espresso

- Setup of Quantum Espresso including necessary libraries
- Writing input SCF files
- Generating input SCF files from CIF files online
- Optimization of wavefunction cutoff
- Optimization of K points via NxNxN convergence method
- Relax and Variable cell relaxation calculation
- Calculation of bulk modulus
- Calculating density of states and integrated density of states and plotting DOS vs Energy
- Plotting Electronic Band Structure
- Calculation of band gap
- Basic quantum physics knowledge and equations of band structure